ISSN 1063-7761, Journal of Experimental and Theoretical Physics, 2017, Vol. 125, No. 6, pp. 1090–1095. © Pleiades Publishing, Inc., 2017.
Original Russian Text © Yu.E. Samoshkina, M.V. Rautskii, E.A. Stepanova, D.S. Neznakhin, N.V. Andreev, V.I. Chichkov, 2017, published in Zhurnal Eksperimental'noi i Teoreticheskoi Fiziki, 2017, Vol. 152, No. 6, pp. 1279–1285.

ORDER, DISORDER, AND PHASE TRANSITION IN CONDENSED SYSTEM

Determination of the Existence Region of a Griffith-like Phase in $Pr_{1-x}Sr_xMnO_3$/YSZ Films

Yu. E. Samoshkina[a,*], M. V. Rautskii[a], E. A. Stepanova[b], D. S. Neznakhin[b], N. V. Andreev[c], and V. I. Chichkov[c]

[a] *Kirensky Institute of Physics, Federal Research Center Krasnoyarsk Scientific Center, Siberian Branch, Russian Academy of Sciences, Krasnoyarsk, 660036 Russia*
[b] *El'tsyn Ural Federal University, Yekaterinburg, 620002 Russia*
[c] *National Research Technological University "MISiS," Moscow, 119049 Russia*
**e-mail: uliag@iph.krasn.ru*

Received May 29, 2017

Abstract—We have studied the temperature dependences of the magnetic susceptibility and the electron magnetic resonance in $Pr_{1-x}Sr_xMnO_3$/YSZ polycrystalline films ($x = 0.2$, 0.4). The paramagnetic properties of samples indicate the presence of short-range-order ferromagnetic correlations above the phase transition temperature (T_c). The existence region of such correlations has been considered using the Griffith theory.

DOI: 10.1134/S106377611712007X

1. INTRODUCTION

The interest in manganites $Ln_{1-x}A_xMnO_3$ (Ln^{3+} stands for a lanthanide and A^{2+} for an alkali-earth ion) has arisen primarily by the effect of colossal magnetoresistance (CMR) typical of these materials. In addition, the phase diagrams of these materials are rich due to closely interrelated spin, orbital, charge, and lattice degrees of freedom [1–3]. The competition of different types of ordering is responsible for the phase separation in manganites and the coexistence of phases with different magnetic and electronic properties. Therefore, the explanation of fundamental of the formation of such phases and their dynamic interaction continues to be an important problem for researchers.

Analysis of magnetic properties of $Ln_{1-x}A_xMnO_3$ manganites in the range $0.2 \le x \le 0.4$ has shown that samples contain as a rule two phases, viz., the ferromagnetic phase below the phase transition point T_c and the paramagnetic phase above T_c [3]. At the same time, inhomogeneity of magnetic states in substituted manganites above their T_c was observed in a large number of publications (see, for example, [4–6]). Such a behavior was considered for the first time by Griffith for randomly diluted Ising ferromagnets, in which a phase in the form of ferromagnetic clusters in a paramagnetic matrix is realized above T_c [7]. Later [8, 9], Griffith's idea was generalized to any disordered magnetic system, including manganites. The Griffith theory was used for manganites for the first time for explaining the experimental data on the CMR, magnetic susceptibility, and heat capacity, which were obtained for $La_{0.7}Ca_{0.3}MnO_3$ compound [10]. It is generally accepted that a Griffith-like phase plays an important role in the CMR formation [10–14]. As noted in [15], the classical Griffith phase should be distinguished from a Griffith-like phase that is formed in substituted manganites because the value of the double-exchange energy in such systems for the Mn^{3+}–Mn^{4+} ion pair is not fixed but depends on external influences.

It is well known that the methods for studying the magnetic resonance are very sensitive to the presence of magnetic impurities. In particular, the electron magnetic resonance (EMR) was used for studying a large number of compositions of substituted manganites [4, 5], including polycrystalline $Pr_{0.6}Sr_{0.4}MnO_3$ samples [6]. We employed the EMR method for investigating polycrystalline $Pr_{1-x}Sr_xMnO_3$ films ($x = 0.2$, 0.4) deposited on an yttrium-stabilized zirconium oxide (YSZ) substrate. Analysis of magnetic properties of such samples performed in [16] showed that the value of T_c for them is much lower than for single crystals. Such a situation implies the presence of phase separation in the samples and the possible detection of ferromagnetic correlations above T_c. In addition, $Pr_{0.8}Sr_{0.2}MnO_3$/YSZ and $Pr_{0.6}Sr_{0.4}MnO_3$/YSZ represent two types of compounds, viz., a ferromagnetic insulator ($x = 0.2$) and a ferromagnetic semiconductor ($x = 0.4$), this allows to investigate the manganites physics more extensively.

2. SAMPLES AND EXPERIMENTAL TECHNIQUE

$Pr_{0.8}Sr_{0.2}MnO_3$ and $Pr_{0.6}Sr_{0.4}MnO_3$ films with thicknesses from 50 to 130 nm were prepared by reactive high-frequency magnetron sputtering in accordance with the facing-target scheme described in [17]. As the working gas, we used the argon–oxygen mixture $Ar/O_2 = 4/1$. The residual pressure in the chamber before sputtering was 3×10^{-6} Torr and the total working pressure in the mixture was 3×10^{-3} Torr. Stoichiometric $Pr_{0.8}Sr_{0.2}MnO_3$ and $Pr_{0.6}Sr_{0.4}MnO_3$ targets were obtained by solid-phase synthesis from Pr_2O_3, SrO, and MnO_2 powders. For the substrate, we used a YSZ(311) single crystal. The substrate temperature during sputtering was 750°C. The chemical composition of the obtained films, which was studied by Rutherford backward scattering, was in correspondence with the declared stoichiometry. The crystalline structure of the samples was studied in [18] and refined for space group *Pnma*. It was found that the structural parameters of the films coincide with the structural data for their bulk analogs [19–22]. The average size of crystallites for $Pr_{0.6}Sr_{0.4}MnO_3$ is 45 nm along the *b* axis and 62 nm along the *a* and *c* axes; for $Pr_{0.8}Sr_{0.2}MnO_3$, it is 31 nm along the *b* axis and 54 nm along the *a* and *c* axes. The texture in the film has not been revealed.

The magnetic susceptibility was measured using the MPMS XL-7 EC SQUID magnetometer in the temperature interval 5–350 K in magnetic fields *H* from 100 to 3000 Oe applied in the plane of the samples. The EMR spectra were recorded on the Bruker E 500 CW spectrometer at frequency $\omega = 9.2$ GHz in the temperature interval 110–320 K.

3. RESULTS AND DISCUSSION

Figure 1 shows the typical temperature dependences of the magnetic susceptibility and its inverse value for two $Pr_{0.8}Sr_{0.2}MnO_3$/YSZ and $Pr_{0.6}Sr_{0.4}MnO_3$/YSZ films obtained in a magnetic field of 100 Oe. The temperature dependence of the inverse susceptibility shows that the value of T_c for the films is quite low as compared to their bulk analogs (Table 1). The value of T_c was determined as the limiting point prior to the growth of $1/\chi$ upon an increase in temperature. It was found that the value of T_c weakly depends on the film thickness. It is well known that the magnetic susceptibility of a homogeneous paramagnetic must obey the Curie–Weiss law, and its inverse value must change linearly with temperature in accordance with the equation $1/\chi = (T - \Theta)/C$, where *C* is the Curie constant and Θ is the Curie–Weiss temperature. It can be seen from Fig. 1 that the inverse susceptibility of the films in the PM region deviates from this dependence, that indicates a change in the effective magnetic moment in this region. Using the linear approximation of a segment of experimental curve $1/\chi(T)$, which is shown in Fig. 1, for each experimental sample, we determined the value of Θ; at arbitrary points T_W taken on the curves, we calculated constant *C* and effective magnetic moment μ_{eff}, which are connected by the formula

$$(\mu_{eff}\mu_B)^2 = 3k_B C/N_A, \quad (1)$$

where $k_B = 1.38 \times 10^{-23}$ J/K is the Boltzmann constant, $\mu_B = 9.274 \times 10^{-24}$ J/T is the Bohr magneton, and $N_A = 6.022 \times 10^{23}$ mol^{-1} is the Avogadro number. In calculating constant *C*, we took into account χ molar value with densities of the samples $\rho_{x=0.2} = 6.667$ g/cm^3 and $\rho_{x=0.4} = 6.469$ g/cm^3. The magnetic parameters calculated for $H = 100$ Oe are given in Table 1. The theoretical value of the effective magnetic moment in the sample was calculated using the expression

$$\mu_{eff}^{th} = \sqrt{(1-x)\mu_{eff}^2(Mn^{3+}) + (1-x)\mu_{eff}^2(Pr^{3+}) + x\mu_{eff}^2(Mn^{4+})}, \quad (2)$$

where $\mu_{eff}(Mn^{3+}) = 4.9\mu_B$, $\mu_{eff}(Mn^{4+}) = 3.87\mu_B$, and $\mu_{eff}(Pr^{3+}) = 3.58\mu_B$. The experimental value of μ_{eff} for $Pr_{1-x}Sr_xMnO_3$/YSZ films turned out to be much higher than the theoretically predicted value (see Table 1), in which the Van Vleck contribution from the Pr^{3+} ions was taken into account [16]. An increase in the magnetic field to 3 kOe gives an even higher value of μ_{eff}. Such a strong discrepancy indicates the presence of FM inclusions in the investigation temperature interval.

To identify FM correlations in the samples above T_c and to determine the region of their existence, we measured the EMR spectra at $T > T_c$, which formed the basis for constructing the temperature dependences of the parameters of the resonance lines. Figure 2 shows typical EMR series of ($d\mathbf{P}/d\mathbf{H}$) spectra in the temperature interval 110–200 K (for $x = 0.2$) and 200–320 K (for $x = 0.4$), which contain the PM region and the region of the FM–PM transition. In the paramagnetic region, an EMR signal should be described by a single symmetric Lorentzian line, and the deviation from this shape may indicate the presence of a ferromagnetic component. As a rule, two resonance lines belonging to the FM and PM components are observed in the paramagnetic region of manganite crystals near their T_c [5, 23], while polycrystalline samples exhibit one resonance line with a deviation from the Lorentzian shape [4, 6]. In the case of poly-

crystalline samples, such a behavior may indicate that the FM and PM resonance lines overlap. In our case, at $T > T_c$, we do not observe an individual line that can be attributed to the FM resonance, thus EMR spectra cannot be described by a single Lorentzian line. Analysis of the EMR spectra was carried out using the standard procedure [4, 6, 24, 25]. The effective g factor was calculated by the formula $g_{eff} = h\nu/\mu_B H_{res}$, where h is the Planck constant, μ_B is the Bohr magneton, ν is the frequency, and H_{res} is the resonant magnetic field. Line width ΔH was determined as the distance between the maximum and minimum on the $dP/dH(H)$ curves. The resonance response intensity was calculated as $I = A^*\Delta H^2$, where A is the amplitude of the dP/dH signal, which is determined by the distance between the maximum and the minimum.

As can be seen from Fig. 3a, a sharp increase in the resonance field by approximately 1.5 times upon a transition through T_c and a further increase in the temperature is characteristic for the studied films, a growth H_{res} slowing down at $T = 145$ and 280 K, after which resonance field attains its maximal value $H_{res} =$ 3248 and 3352 Oe at $T = 170$ and 300 K for $x = 0.2$ and 0.4, respectively. These temperature dependences of the resonance field correspond to the temperature dependences of g_{eff} value shown in Fig. 3b. It should be noted that g_{eff} has a high value (approximately 2.75) in the vicinity of T_c of the samples, which then decreases with increasing temperature and becomes close to 2 at $T = 200$ and 300 K for $x = 0.2$ and 0.4, respectively. These results indicate that the samples exhibit the "normal" PM behavior only at temperatures much higher than their T_c values.

The anomalous PM behavior is more obvious, on the basis of the temperature dependence of the resonance line width ΔH (Fig. 4). As can be seen from the figure, ΔH value is not a monotonic function of temperature, and demonstrates a minimum at temperatures $T_{min} = 145$ and 295 K for $x = 0.2$ and 0.4, respectively, which is much higher than the values of T_c for the films. It should be noted that such a behavior of ΔH at $T > T_c$ is typical for manganites and was observed earlier for various compositions [4, 6, 24, 25]. It is known that the resonance line width mainly depends on the force of interaction between the spins of magnetic ions and the relaxation mechanism. In the FM region, the broadening of the resonance line during cooling is usually attributed to slowdown of spin fluctuations due to increase of the exchange interaction. For such systems as manganites, the "normal" PM region is characterized by line broadening upon heating, which is explained by the spin–lattice relaxation and the presence of magnetic polarons. Thus, the observed increase in ΔH upon cooling in the interval $T_c < T < T_{min}$ also indicates the coexistence of the FM and PM regions in the samples.

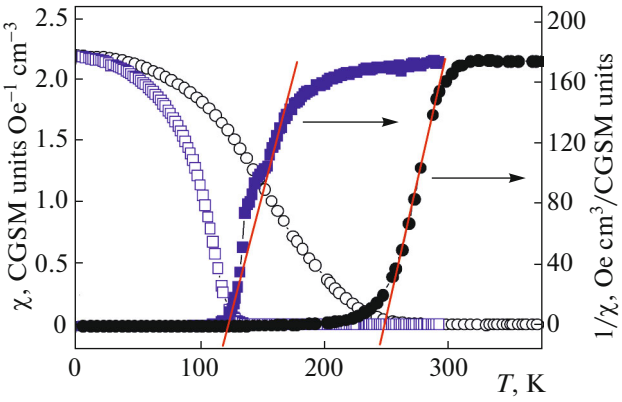

Fig. 1. (Color online) Temperature dependences of the magnetic susceptibility and its inverse value for $Pr_{1-x}Sr_xMnO_3$/YSZ films ($d \sim 100$ nm), measured during cooling in magnetic field $H = 100$ Oe; (squares) $Pr_{0.8}Sr_{0.2}MnO_3$; (circles) $Pr_{0.6}Sr_{0.4}MnO_3$.

The intensity of the resonance signals, which is presented in Fig. 5 as a function of temperature, is proportional to the magnetic susceptibility of the films. The temperature dependences of its inverse value are also shown in Fig. 5, which demonstrates the absence of a clear linear dependence at temperatures above T_c. If, however, we try to describe the data by a linear function, the temperature values at which deviations are observed will be 155 and 295 K for $x = 0.2$ and 0.4, respectively, which are close to the T_{min} values.

In a number of publications [4, 5, 10, 25], the peculiarities of the magnetic behavior of substituted manganites above their T_c (nonlinear dependence $1/\chi(T)$, large values of μ_{eff}, and asymmetry of the EMR signal) are treated as features of a Griffith-like phase. It should be noted in this connection that this phase for $Ln_{1-x}A_xMnO_3$ can be observed in the temperature range up to the maximal value of T_c of the system [26]. It is known that the maximal value of $T_c \sim 370$ K is

Table 1. Experimental data for $Pr_{1-x}Sr_xMnO_3$/YSZ films ($d \sim 100$ nm), obtained in a magnetic field of 100 Oe

	$x = 0.2$	$x = 0.4$
T_c, K	115	215
	158 [20] polycrystal	300 [21] single crystal
	170 [19] polycrystal	305 [22] polycrystal
Θ, K	119	246.5
T_W, K	142	275
C, cm^3 K/mol	157.23	117.33
μ_{eff}^{exp}, μ_B	11.21	9.68
μ_{eff}^{th}, μ_B	5.70	5.30
T_G, K	145	295

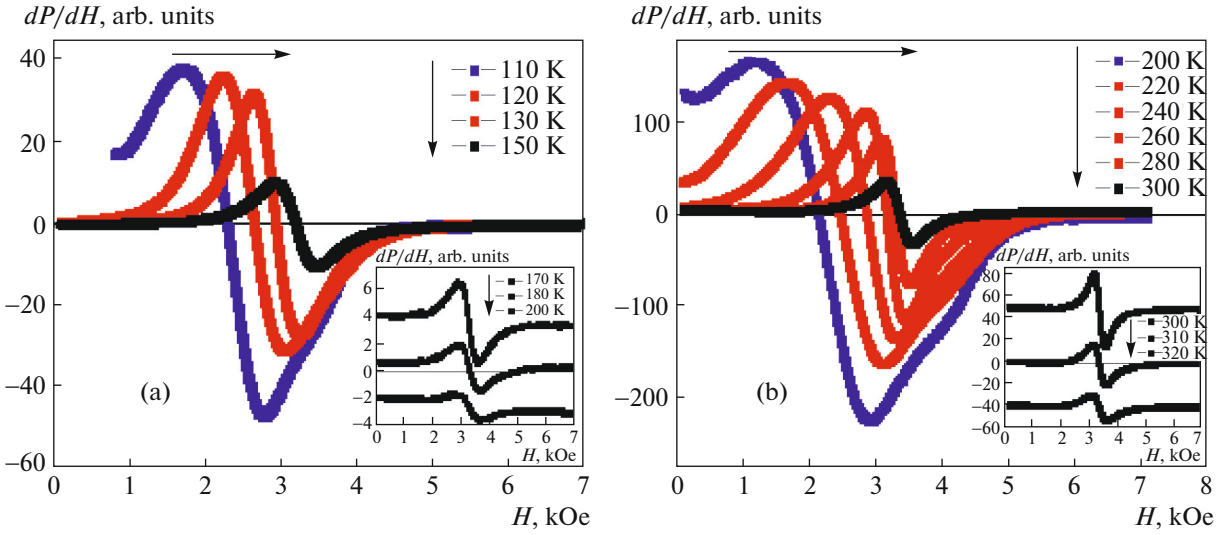

Fig. 2. (Color online) Temperature dependences of EMR spectra: (a) $Pr_{0.8}Sr_{0.2}MnO_3$/YSZ (d ~ 100 nm); (b) $Pr_{0.6}Sr_{0.4}MnO_3$/YSZ (d ~ 130 nm).

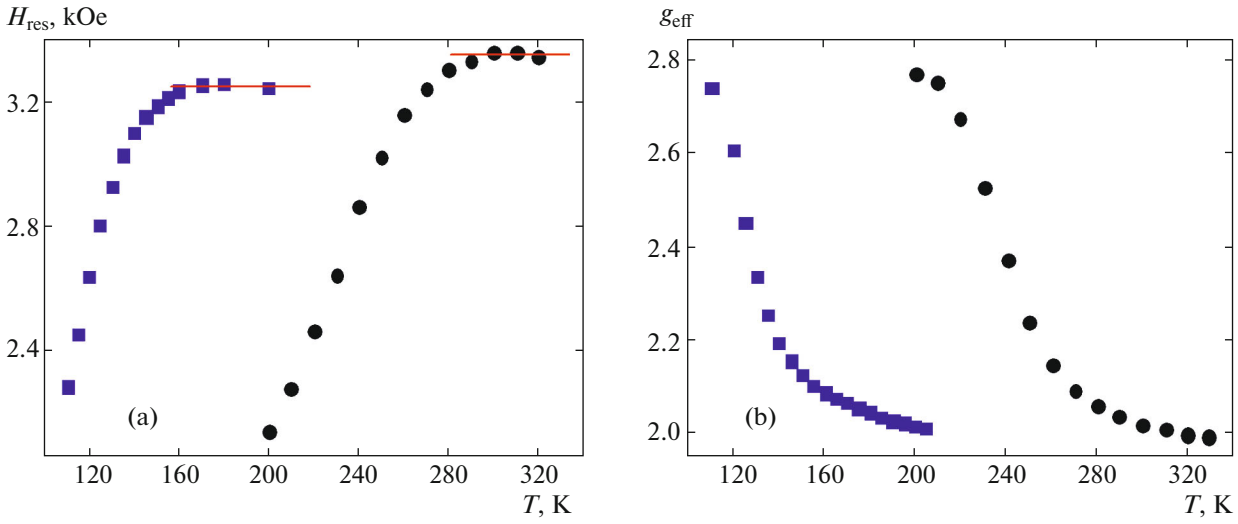

Fig. 3. (Color online) Temperature dependence of (a) magnetic resonance field and (b) effective g factor for $Pr_{1-x}Sr_xMnO_3$/YSZ: (squares) $Pr_{0.8}Sr_{0.2}MnO_3$; (circles) $Pr_{0.6}Sr_{0.4}MnO_3$.

observed for manganite $La_{0.7}Sr_{0.3}MnO_3$. According to the phase diagram [27] and recent magnetic studies [21, 22], the high value of T_c ~ 305 K in series $Pr_{1-x}Sr_xMnO_3$ of substituted manganites corresponds to samples with $x = 0.4$. However, the presence of FM correlations was also established for bulk $Pr_{0.6}Sr_{0.4}MnO_3$ polycrystals in temperature interval $T =$ 305–330 K [6]. Magnetic measurements show that in our case, the films have values of T_c lower then in single crystals (see Table 1). The magnetic resonance data in this case indicate the presence of an FM signal in the experimental samples above the mentioned transition temperature, but not exceeding $T =$ 305 K. Therefore, the observed magnetic behavior of $Pr_{1-x}Sr_xMnO_3$/YSZ films in the temperature interval $T_c < T < T_{min}$ is successfully explained using the Griffith theory that predicts the existence of short-range-order FM correlations in the PM region. According to the $\Delta H(T)$ dependence shown in Fig. 5, ferromagnetic correlations disappear above T_{min}, and the system demonstrates the "normal" PM behavior. As the sample is cooled below T_{min}, regions of the short-range FM order appearing in the PM region increase upon cooling and form a long-range FM order after passing through T_c.

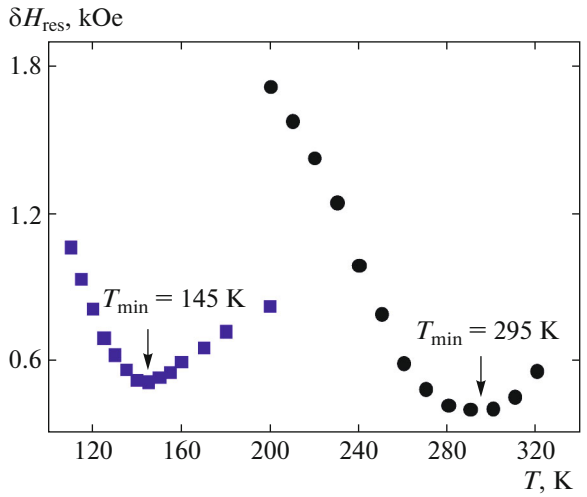

Fig. 4. (Color online) Temperature dependences of the resonance line width for $Pr_{1-x}Sr_xMnO_3$/YSZ: (squares) $Pr_{0.8}Sr_{0.2}MnO_3$; (circles) $Pr_{0.6}Sr_{0.4}MnO_3$.

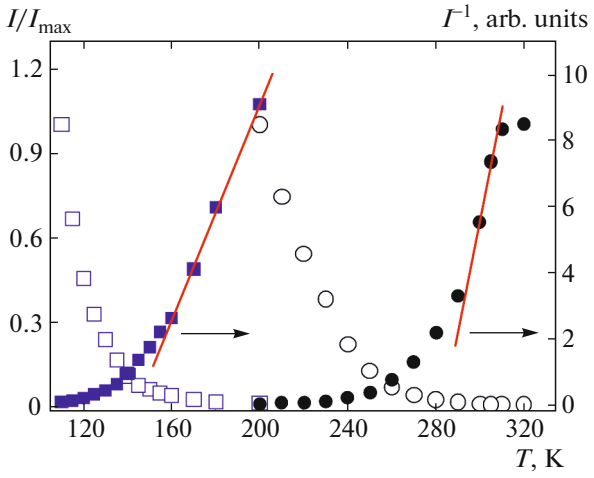

Fig. 5. (Color online) Temperature dependences of the resonance signal intensity and its inverse value for $Pr_{1-x}Sr_xMnO_3$/YSZ: (squares) $Pr_{0.8}Sr_{0.2}MnO_3$; (circles) $Pr_{0.6}Sr_{0.4}MnO_3$.

The existence region of a Griffith-like phase in the studied films was determined proceeding from the temperature dependence of ΔH; the Griffith temperature T_G was found to be equal to T_{min}. It is known that inhomogeneous PM state with inclusions of magnetic polarons [12, 28], which can elevate the value of H_{res} and, accordingly, g_{eff}, can be detected in manganites even above T_G. It should be noted that the boundaries of this region weakly depend on the thickness of the films as in the case of T_c.

Wide boundaries of the Griffith-like phase were determined earlier for $La_{1-x}(Sr/Ba)_xMnO_3$ with x varying from 0.075 to 0.2 above their T_c [5, 23]. It was assumed that the formation of FM correlations in the PM region, which is a form of phase separation, is associated with the parameter of disorder caused by Sr/Ba ions. In the case of $Pr_{1-x}Sr_xMnO_3$/YSZ films, the Griffith-like phase is also observed in wide temperature intervals that do not exceed, however, T_c of analogous single crystals. Wide boundaries of this phase and their shift towards lower temperatures are obviously due to the displacement of the phase separation boundaries in the samples. As a rule, phase separation is divided into internal and external; the internal separation is associated with the type of the materials with a tendency to inhomogeneity, while the external separation appears due to external perturbations (e.g., due to the strain exerted by the substrate on the film) [29, 30]. The Griffith-like phases observed in manganite single crystals should probably be attributed to internal phase separation in the material. In the case of thin films, external strain considerably affect their physical properties. Taking into account the fact that $Pr_{1-x}Sr_xMnO_3$/YSZ films turned out to be polycrystalline due to considerable mismatch of the lattices of the manganite and the film substrate, it can be concluded that is no strain between the substrate and the film in the initial sample. We studied earlier $La_{0.7}Sr_{0.3}MnO_3$/YSZ films that also exhibited low value of $T_c \sim 300$ K [31]. According to electron microscopy data, the crystallites in the samples were characterized by a random orientation in the plane and were superimposed to form several layers; we also observed moirs and other structural peculiarities. Thus, we can propose that the observed phase separation in $Pr_{1-x}Sr_xMnO_3$/YSZ films is associated with the strain emerging between the lattices of crystallites constituting the samples. This was confirmed by magnetic data obtained for $Pr_{0.7}Sr_{0.3}MnO_3$ films deposited on sapphire [32]. Manganite and sapphire also exhibit a considerable mismatch of the crystal lattices, and the resultant polycrystalline film is characterized by a lower value of $T_c \sim 200$ K as compared to the single crystal with T_c approximately equal to 250 K. The internal phase separation in film materials cannot be ruled out, but the external separation plays a dominant role.

It should be noted that considering the presence of a Griffith-like phase in the samples as the key to the formation of the CMR, we found that dielectric films are not an exception. The magnetoresistance effect is observed in these films also in strong magnetic fields [33]. In some cases, the dielectric films demonstrate a metal–insulator transition in magnetic fields on the order of 50–100 kOe [33, 34].

4. CONCLUSIONS

It can be concluded based on the data on magnetic susceptibility and electron magnetic resonance that polycrystalline $Pr_{1-x}Sr_xMnO_3$/YSZ films ($x = 0.2$, $x = 0.4$) of thickness 50–130 nm at temperatures above

their T_c (115 K and 215 K, respectively) contain a Griffith-like phase in the form of ferromagnetic correlations of the short-range order in the paramagnetic region. The existence region of this phase has been determined for each film proceeding from the temperature dependence of the EMR line width and is limited by temperature T_G equal to 145 K for $x = 0.2$ and 295 K for $x = 0.4$. The low value of T_c of the films and, accordingly, wide boundaries of the existence region of the Griffith-like phase in the samples are due to a shift of the phase separation boundaries, which is induced by the strain between the lattices of individual crystallites constituting the films. The presence of internal phase separation in the films is not ruled out, but we emphasize the dominant role of the external phase separation, which also explains the weak dependence of T_c and the boundaries of the Griffiths-like phase on the film thickness.

ACKNOWLEDGMENTS

This study was supported by the Russian Foundation for Basic Research (project no. 16-32-00209mol_a) and the Council for Grants from the President of the Russian Federation (NSh-7559.2016.2). E. A. Stepanova and D. S. Neznakhin were supported by the RF Ministry of Education and Sciences (State target no. 3.61212017/8.9).

REFERENCES

1. J. M. D. Coey, M. Viret, and S. von Molnar, Adv. Phys. **48**, 167 (1999).
2. A.-M. Haghiri-Gosnet and J.-P. Renard, J. Phys. D: Appl. Phys. **36**, R127 (2003).
3. M. S. Dunaevskii, Phys. Solid State **46**, 193 (2004).
4. X. J. Liu, E. Y. Jiang, Z. Q. Li et al., J. Magn. Magn. Mater. **305**, 352 (2006).
5. R. M. Eremina, I. V. Yatsyk, Ya. M. Mukovskii, H. A. Krug von Nidda, and A. Loidl, JETP Lett. **85**, 51 (2007).
6. R. Thaljaoui, W. Boujelben, M. Pękała, et al., J. Alloys Compd. **526**, 98 (2012).
7. R. Griffiths, Phys. Rev. Lett. **23**, 17 (1969).
8. A. J. Bray and M. A. Moore, J. Phys. C **15**, L765 (1982).
9. A. J. Bray, Phys. Rev. Lett. **59**, 586 (1987).
10. M. B. Salamon, P. Lin, and S. H. Chun, Phys. Rev. Lett. **88**, 197203 (2002).
11. J. Burgy, M. Mayr, V. Martin-Mayor, et al., Phys. Rev. Lett. **87**, 277202 (2001).
12. E. Dagotto, New J. Phys. **7**, 67 (2005).
13. J. Tao, D. Niebieskikwiat, Q. Jie, et al., Proc. Natl. Acad. Sci. USA **108**, 20941 (2011).
14. S. Rößler, S. Ernst, B. Padmanabhan, et al., Europhys. Lett. **83**, 17009 (2008).
15. V. N. Krivoruchko, J. Low Temp. Phys. **40**, 586 (2014).
16. Yu. E. Samoshkinaa, I. S. Edelman, E. A. Stepanova, et al., J. Magn. Magn. Mater. **428**, 43 (2017).
17. Y. Hoshi, M. Kojima, M. Naoe, et al., Electron. Commun. Jpn., Part. IV **65**, 91 (1982).
18. I. Edelman, Yu. Greben'kova, A. Sokolov, et al., AIP Adv. **4**, 057125 (2014).
19. W. Boujelben, A. Cheikh-Rouhou, M. Eellouze, et al., J. Phase Trans. **71**, 127 (2000).
20. N. Rama, V. Sankaranarayanan, and M. S. Ramachandra Rao, J. Appl. Phys. **99**, 08Q315 (2006).
21. S. Rößler, S. Harikrishnan, U. K. Rößler, et al., Phys. Rev. B **84**, 184422 (2011).
22. R. Thaljaoui, W. Boujelben, M. Pękała, et al., J. Supercond. Nov. Magn. **26**, 1625 (2013).
23. J. Deisenhofer, D. Braak, H.-A. Krug von Nidda, et al., Phys. Rev. Lett. **95**, 257202 (2005).
24. C. Autret, M. Gervais, F. Gervais, et al., Solid State Sci. **6**, 815 (2004).
25. L. Chen, J. Fan, W. Tong, et al., Sci. Rep. **6**, 14 (2016).
26. W. Jiang, X. Zh. Zhou, G. Williams, et al., Phys. Rev. B **77**, 064424 (2008).
27. C. Martin, A. Maignan, M. Hervieu, et al., Phys. Rev. B **60**, 12191 (1999).
28. S. Methfessel and D. Mattis, in *Handbook of Physics*, Ed. by H. P. J. Wijn (Springer, Berlin, 1968; Mir, Moscow, 1972), Vol. 18, part 1.
29. E. Dagotto, T. Hotta, and A. Moreo, Phys. Rep. **344**, 1 (2001).
30. M. Uehara, S. Mori, C. H. Chen, et al., Nature **399**, 560 (1999).
31. Yu. E. Greben'kova, A. E. Sokolov, E. V. Eremin, I. S. Edel'man, D. A. Marushchenko, V. I. Zaikovskii, V. I. Chichkov, N. V. Andreev, and Ya. M. Mukovskii, Phys. Solid State **55**, 842 (2013).
32. H. Wang, K. Su, S. Huang, and W. Tan, J. Mater. Sci.: Mater. Electron. (2017). doi 10.1007/s10854-017-6917-3
33. B. Padmanabhana, S. Elizabetha, H. L. Bhata, et al., J. Magn. Magn. Mater. **307**, 288 (2006).
34. A. Hassen, J. Korean Phys. Soc. **52**, 98 (2008).

Translated by N. Wadhwa